Acta Oceanol. Sin., 2016, Vol. 35, No. 10, P. 1–10
DOI: 10.1007/s13131-016-0922-x
http://www.hyxb.org.cn
E-mail: hyxbe@263.net

Arctic sea ice thickness changes in terms of sea ice age

BI Haibo[1]*, FU Min[2], SUN Ke[3], LIU Yilin[1], XU Xiuli[2], HUANG Haijun[1]

[1] Key Laboratory of Marine Geology and Environment, Institute of Oceanology, Chinese Academy of Sciences, Qingdao 266071, China

[2] National Marine Environmental Forecasting Center, Beijing 100081, China

[3] The First Institute of Oceanology, State Oceanic Administration, Qingdao 266061, China

Received 15 August 2015; accepted 31 December 2015

Abstract

In this study, changes in Arctic sea ice thickness for each ice age category were examined based on satellite observations and modelled results. Interannual changes obtained from Ice, Cloud, and Land Elevation Satellite (ICESat)-based results show a thickness reduction over perennial sea ice (ice that survives at least one melt season with an age of no less than 2 year) up to approximately 0.5–1.0 m and 0.6–0.8 m (depending on ice age) during the investigated winter and autumn ICESat periods, respectively. Pan-Arctic Ice Ocean Modeling and Assimilation System (PIOMAS)-based results provide a view of a continued thickness reduction over the past four decades. Compared to 1980s, there is a clear thickness drop of roughly 0.50 m in 2010s for perennial ice. This overall decrease in sea ice thickness can be in part attributed to the amplified warming climate in north latitudes. Besides, we figure out that strongly anomalous southerly summer surface winds may play an important role in prompting the thickness decline in perennial ice zone through transporting heat deposited in open water (primarily via albedo feedback) in Eurasian sector deep into a broader sea ice regime in central Arctic Ocean. This heat source is responsible for enhanced ice bottom melting, leading to further reduction in ice thickness.

Key words: sea ice, thickness, age, ICESat, PIOMAS

Citation: Bi Haibo, Fu Min, Sun Ke, Liu Yilin, Xu Xiuli, Huang Haijun. 2016. Arctic sea ice thickness changes in terms of sea ice age. Acta Oceanologica Sinica, 35 (10): 1–10, doi: 10.1007/s13131-016-0922-x

1 Introduction

Polar sea ice is one of the most visible components corresponding to climate changes. Along with a continued coverage decline (Comiso et al., 2008), a thinning trend was also observed over the Arctic Ocean sea ice (Kwok and Rothrock, 2009). The decrease in ice thickness has extensive meanings in terms of heat and momentum exchanges between ocean and atmosphere. If ice pack became thinner, more heat would escape from warm ocean water into atmosphere above.

The overall thinning Arctic sea ice over the past several decades has been documented in previous studies. Evidences of a significant decline in Arctic sea ice thickness are provided by such studies which analyzed submarine records despite that they are limited both in time and space (Rothrock et al., 2008). Although short, satellite altimeters (such as ICESat), which have an unique potential to regularly acquire much more extensive measurements of polar sea ice, is used to investigate near Arctic-wide ice thickness changes. For instance, Kwok and Rothrock (2009) unveiled a notable decline by 1.8 m of Arctic sea ice thickness by comparing ICESat-derived thickness with historical submarine records. In addition, well-assessed PIOMAS modelled results are a useful data to study long-term changes (Zhang and Rothrock, 2003).

The overall mass loss in the Arctic sea ice cover is primarily attributable to climate changes (Vinnikov et al., 1999; Laxon et al., 2003; Johannessen et al., 2004). Dynamic (such as atmospheric circulation (Deser and Teng, 2008; Ogi et al., 2010) and ocean currents (Shimada et al., 2006; Alexeev et al., 2013)) and thermodynamic (melting and freezing (Markus et al., 2009; Stroeve et al., 2014)) activities in Arctic atmosphere and Ocean causes the replacement of older multiyear (MY) ice by younger ice (Maslanik et al., 2007; Maslanik et al., 2011), decline in thickness (Rothrock et al., 2008; Kwok and Rothrock, 2009) and ice concentration (Comiso et al., 2008), as well as increasing fraction of melt pond (Schröder et al., 2014), etc. Here we concentrate on the changes in thickness of sea ice in terms of a given age, which has not been extensively examined so far but serves as an important indicator allowing us to comprehensively understand what is happening over the Arctic Ocean sea ice cover.

In the present study, the thickness changes of all ice age groups from 1-year through 5+ (i.e., older than five years) is investigated using both ICESat-derived thickness and PIOMAS modelled thickness. Observations from recently launched SMOS and Cryosat-2 satellites are not used owing to its large uncer-

Foundation item: The National Natural Science Foundation of China under contract No. 41406215; the Postdoctoral Science Foundation of China under contract No. 2014M561971; the Open fund for the Key Laboratory of Marine Geology and Environment, Institute of Oceanology, Chinese Academy of Sciences under contract No. MGE2013KG07; the Chinese Polar Environment Comprehensive Investigation and Assessment Program, State Oceanic Administration under contract Nos CHINARE2014-03-01 and CHINARE2014-04-03.
*Corresponding author, E-mail: bhb@qdio.ac.cn

tainty and further assessment is necessary. While the ICESat-derived sea ice thickness is utilized to examine the short-term (2003–2008) interannual variations of ice thickness, PIOMAS thickness is employed to investigate the decadal changes since 1980s. Moreover, the likely causes connected to sea ice thickness changes, such as warm climate and summer winds, were discussed in this paper.

2 Data

In this study, we make use of sea ice age and thickness data (including those from satellite altimeter measurements of ICESat and from PIOMAS model) to investigate the interannual and decadal thickness changes with respect to each ice age category. Synoptic information about the datasets used is summarized in Table 1. Detailed descriptions about these data are given in the corresponding texts (Section 2.1–2.4). Exemplary maps of ICESat and PIOMAS ice thickness as well as age fields are shown in Fig. 1. Given that extensive validation show a good consistency between ICESat-derived sea ice thickness and *in situ* measurements (Kwok et al., 2009), we only conduct an assessment for the PIOMAS thickness (Section 2.2).

Table 1. Data used in this study

Data used	Representative month	Time period	Reference	Grid cell size	Provider
Ice age	depending on thickness fields used	depending on thickness data	Maslanik et al. (2007) Maslanik et al. (2011)	12.5 km	University of Colorado
ICESat-derived sea ice thickness	mid-February to mid-March or mid-March to mid-April	2004–2009	Kwok et al. (2009)	25 km	NASA JPL
PIOMAS modelled sea ice thickness	March	1980–2015	Zhang and Rothrock (2003) Schweiger et al. (2011)	25 km	University of Washington
Sea ice extent	September	1978–2014	Fetterer et al. (2002)	25 km	NSIDC
NCEP/Reanalysis surface air temperature and winds	winter (October–May) and summer (June–September)	1980–2015	Kalnay et al. (1996)	2.5°×2.5°	NOAA

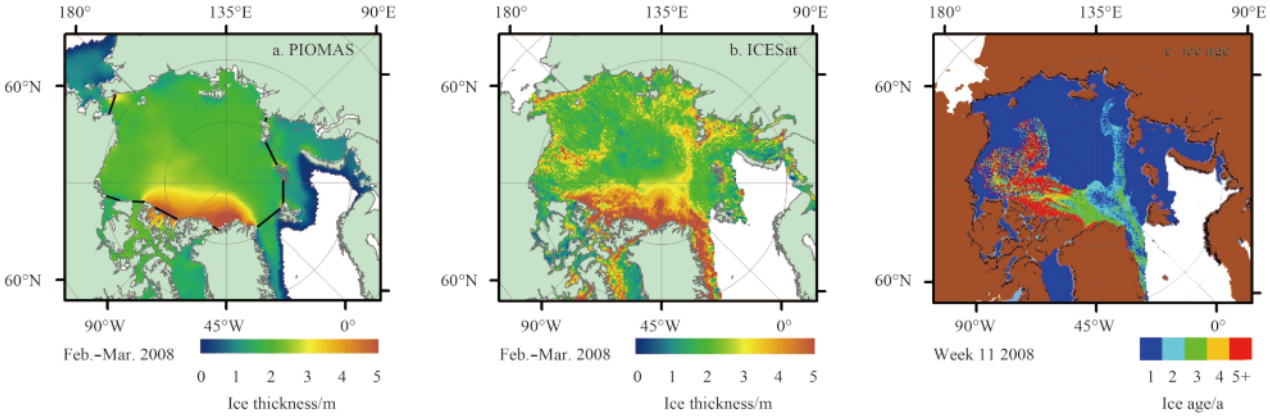

Fig. 1. Representative maps for PIOMAS sea ice thickness (a) and ICESat-derived sea ice thickness (b) as well as contemporary ice age (c). The date of these maps is on February–March 2008 following the summer/autumn period of dramatic ice loss observed in 2007. The black lines as marked in Fig. 1a correspond to the fluxgate of sea ice exiting the Arctic Ocean. These lines and neighboring coasts are connected to form the boundaries of our study area of the Arctic Ocean, within which mean sea ice thickness is calculated in terms of sea age.

2.1 *ICESat-derived sea ice thickness*

According to the Archimedes buoyancy principle, sea ice thickness can be derived from freeboard profiles made by the ICESat Geoscience Laser Altimeter System (GLAS) instrument (Kwok and Cunningham, 2008; Zwally et al., 2008). Sea ice thickness converted from ICESat freeboard now is now public available and can be acquired from the National Snow and Ice Data Center (NSIDC) in Boulder, Colorado, which is originally derived by Yi and Zwally (2014). The preliminary sea ice thickness has a nominal footprint of 170 m along the track and the gridded product has a cell size of 25 km.

Details with regard to conversion from ICESat-derived freeboard to thickness were described in several published studies (Zwally et al., 2002; Kwok and Cunningham, 2008; Zwally et al., 2008). The following relationship (Eq.(1)) is used to conduct the freeboard/thickness conversion (Zwally et al., 2008; Kwok et al., 2009):

$$h_{\mathrm{i}} = \frac{\rho_{\mathrm{w}}}{\rho_{\mathrm{w}} - \rho_{\mathrm{i}}} f_{\mathrm{b}} - \frac{\rho_{\mathrm{w}} - \rho_{\mathrm{s}}}{\rho_{\mathrm{w}} - \rho_{\mathrm{i}}} h_{\mathrm{s}}, \tag{1}$$

where f_{b} is the ICESat-measured freeboard. Snow depth (h_{s}) was obtained from climatology (Warren et al., 1999). Constant were used for ice (ρ_{i}=915.1 kg/m^3) and open water (ρ_{w}=1 024 kg/m^3) densities (Zwally et al., 2008). For the density of snow (ρ_{s}), we follow in a seasonal variability illustrated by Kwok and Cunningham (2008), with a value of 250 kg/m^3 and 320 kg/m^3 for the investigated ICESat autumn and winter campaigns, respectively. Further knowledge about the data processing procedure about freeboard derivation and thickness computation, the reader can refer to the technical document available at NSIDC (http://nsidc.org/data/docs/daac/nsidc0393_arctic_seaice_freeboard/index.html).

In this study we make use of the binary Gridded product (with a grid cell size of 25 km on a polar stereographic projection) of ICESat-derived sea ice thickness provided by NSIDC. The data are available with a ".img" format that can be mapped and pro-

cessed using ENVI+IDL and ArcGIS softwares. The gridded thickness points to an average of all the ICESat-derived thickness dropped into that grid cell over one ICESat operational campaign. Typically, an ICESat campaign spans a time range of roughly one month, generally between mid-October and mid-November (hereafter referred to as ON record) in autumn and mid-February and mid-March or mid-March to mid-April (hereafter referred to as FMA record) in winter. In particular, the winter campaigns in 2007 spans a time period of between mid-March and mid-April (hereafter referred to as 07MA). The designations and actual time ranges for the selected ICESat campaigns are listed in Table 2. Altogether, six winter and five autumn campaigns of ICESat-derived gridded sea ice thickness data between 2003 and 2008 were explored here. Spreen (2008) made a detailed introduction about the data gridding procedure and the grid product can be obtained via ftp://sidads.colorado.edu/pub/DATASETS/NSIDC0393_GLAS_SI_Freeboard_v01/glas_seaice_grids/.

Table 2. Time range of selected autumn and winter ICESat campaigns

ICESat Campaign	Time range
03FM	20 February to 29 March 2003
03ON	18 October to 19 November 2003
04FM	17 February to 21 March 2004
04ON	3 October to 8 November 2004
05FM	17 February to 24 March 2005
05ON	21 October to 24 November 2005
06FM	22 February to 28 March 2006
06ON	25 October to 27 November 2006
07MA	12 March to 14 April 2007
07ON	2 October to 5 November 2007
08FM	17 February to 21 March 2008

To further examine the quality of used ICESat-derive sea ice thickness that is available through_ftp://sidads.colorado.edu/pub/DATASETS/NSIDC0393_GLAS_SI_Freeboard_v01/glas_seaice_vectors/, it was evaluated by comparison with measurements from a submarine (15 November 2005) and four moorings belonging to Beaufort gyre experiment project (BGEP) (2003–2008). The track of the cross-Arctic submarine cruise and the sites of the four moorings have been included in Fig. 4. ICESat-derived thickness fields that are spatial-temporally close (within one day in time and 200 km in distance) to *in situ* measurements are finding out. Following Kwok et al. (2009), ice draft (=ice thickness–freeboard height) is utilized in our comparison. As shown in Fig. 2, comparative results reveal a mean bias of 0.06 m with an uncertainty of 0.38 m indicating a relatively good agreement between ICESat and *in situ* measurements.

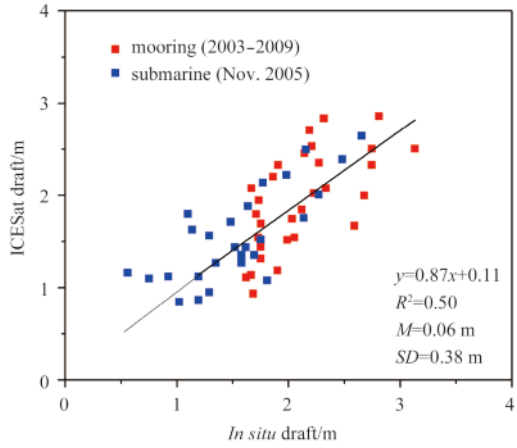

Fig. 2. Evaluating ICESat-derived ice drafts using submarine (black) and mooring measurements (red). Equations of a least square fitted line, squared correlation coefficient (R^2), mean (M) and standard deviation of the differences (SD) are also added.

2.2 *PIOMAS modelled sea ice thickness*

PIOMAS that was developed in the University of Washington provides simulated ice thickness data of a much longer period (1978–2015) (Zhang and Rothrock, 2003) (http://psc.apl.washington.edu/zhang/IDAO/data_piomas.html.), enabling us to examine how the sea ice thickness in the Arctic Ocean has varied over a decadal scale. The model results have been evaluated with various data from submarine record to satellite measurements (Schweiger et al., 2011). Overall, it performs well in reproducing observations, with negligible mean bias and relatively large uncertainties of 0.27–1.17 m though. However, the largest uncertainties of 1.17 m only appeared in limited field measurements near the North Pole and in the Barents Sea, Greenland Sea which has been excluded in our computation of mean thickness. Substantial submarine record covering a major part of the central Arctic Ocean shows a mean bias of 0.17 m. Moreover, EM sounding measurements showed a better agreement with PIOMAS thickness, with a mean bias of zero and uncertainty of only 0.27 m.

Here we further evaluate the PIOMAS thickness using ICESat-derived thickness of NSIDC. A pixel-to-pixel comparison was carried out and the scatterplot is shown in Fig. 3. The linearly fitted

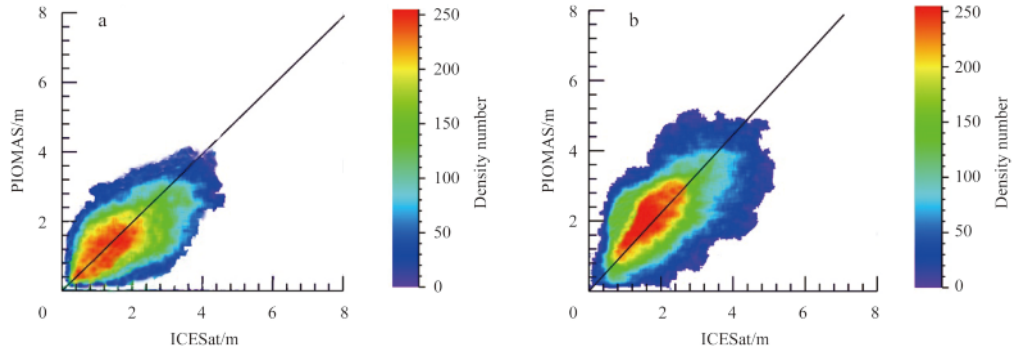

Fig. 3. Pixel-to-pixel comparisons between ICESat and PIOMAS thickness during the ON (a) and FMA (b) period over 2003–2008. The blue-to-red color represents the density number of data pairs. Linearly fitted line (black) is also shown.

lines: y=0.96x for ON period (Fig. 3a) and y=0.98x for FMA period (Fig. 3b) suggest overall slightly smaller PIOMAS thicknesses relative to ICESat thicknesses. The mean bias between the two data is small (–0.01 m) while the standard deviation of the difference (0.6 m for FMA and 0.4 m for ON) between the two data is moderate, but within the above-mentioned uncertainty range. Additionally, our results in Fig. 7 suggest that there is an excellent agreement (no less than 0.2 m) between ICESat and PIOMAS thickness in terms of averaged fields for each ice age category (detailed quantitative description is given in texts of Section 4.2).

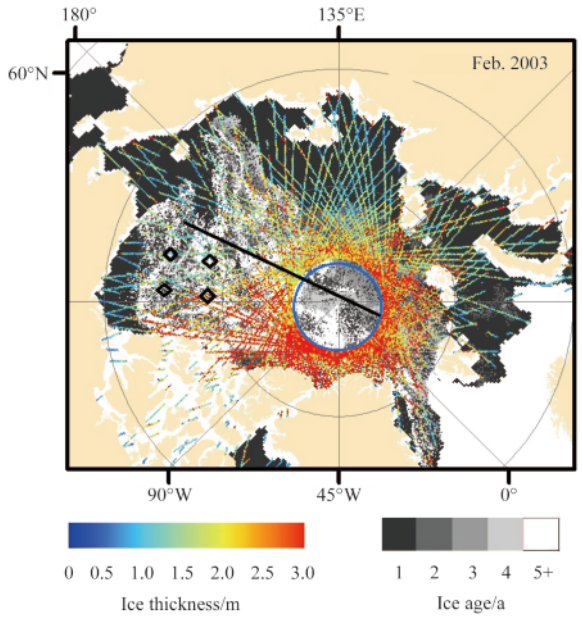

Fig. 4. Composite maps with ICESat-derived ice thickness (contour lines) overlaid on ice age fields (background gray-to-white color) in February 2003. The observational hole north of 86°N of ICESat is marked by the blue circle. The black bold line cross the central Arctic Ocean represents the submarine track mentioned in Section 2.1 and the four black diamond symbols correspond to the locations of four BGEP moorings in the Beaufort Sea region.

2.3 *Ice age data*

The usefulness of the ice age data have been broadly examined in several studies (Rigor and Wallace, 2004; Maslanik et al., 2007, 2011). Ice age data (available from 1979 through the present) available in NSIDC is derived by combining ice drift and ice extent data, both retrieved from satellite-based passive microwave measurements (Tschudi et al., 2014). In their manipulation, an ice grid with ice concentration of exceeding 15% is treated as a free ice floe that floats in a Lagrangian mechanism and can be tracked by following the sea ice drift trajectory. Accordingly, newly formed ice will become a 2-year ice or multi-year ice (older than 2-year) gains an additional year if the tracked ice grid survives one summer melt season. An exemplary map of ice age is presented in Fig. 1c.

2.4 *Ancillary data*

In analyzing the associated causes of a thinner Arctic Ocean sea ice (Section 5.2.3), September sea ice extent (defined as the area covered by ice cover with an ice concentration of larger than 15%) calculated based on ice concentration is used to discuss our results. Ice concentration data (Fetterer et al., 2002) is derived from multiple passive microwave radiometer observations, such as observations from Nimbus-7 SMMR and DMSP SSM/I and SSMIS series, using the NASA Team algorithm. More details about how to calculate sea ice extent is described in http://nsidc.org/data/g02135. In addition, surface air temperature and summer wind anomaly fields in north high latitudes are used to explain our findings. These data were obtained from the NCEP/Reanalysis product (Kalnay, 1996), available at http://www.esrl.noaa.gov/psd/cgi-bin/data/timeseries/timeseries1.pl.

3 Methods

Sea ice thickness and age are the primary data sources to derive sea ice thickness changes in dependent on ice age. However, the grid cell size of ice thickness and age fields is different (Table 1). The grid cell size of ice age data is roughly 12.5 km, whereas the gridded ICESat thickness and PIOMAS modeled thickness has resolution of approximately 25 km. Therefore, these data should be spatially matched before establishing a robust association between ice thickness and ice age.

An example of spatially co-registered map is shown in Fig. 4 with ICESat thickness on February 2003 overlaid on ice age fields of the same period (not shown for PIOMAS thickness). The interpolated thickness fields (as shown in Fig. 5) are used in the computation of mean sea ice thickness for ice with different ages. The incompatibility in pixel size (25 km vs. 12.5 km) between ice thickness and age fields can be reduced following the technique proposed by Maslanik et al.(2007) who calculated the fraction of each age category within a grid of thickness field. That is, the grid size of a thickness field (25 km) contains 2×2 12.5 km grids of ice age and the fraction of each ice age category for a thickness grid is calculated as N/4, where N represents the number of a particular age within the corresponding thickness grid. Then, mean thickness for an ice category is estimated using only thickness cells that contained at least 75% (or 3/4) ice of a particular age. Note that Maslanik et al. (2007) only presented the changes of average thickness for each ice age category over the 2003–2008 period, we provide the interannual variability of average thickness over the short period of 2003–2008 as well as decadal variability since the 1980s.

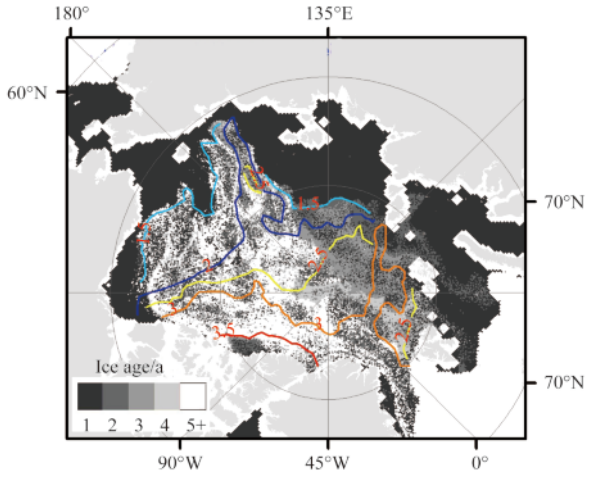

Fig. 5. Interpolated sea ice thickness fields (contour lines) from ICESat-derived gridded sea ice thickness in February 2003 (as shown in Fig. 4). The background gray-to-white color represents ice age fields.

4 Results

4.1 *ICESat-based Arctic sea ice thickness changes*

Figure 6 shows the acquired mean thickness changes in terms of sea ice age during ICESat winter (Fig. 6a) and autumn (Fig. 6b) periods. Typically, the two plots show general increases in ice thickness from 1-year ice through 5+ ice (from 1.45 m to 2.6 m for ON period and from 1.8 m to 3.2 m for FM period, respectively). Interanually, there is a general decrease in winter sea ice thickness from 2003 (red line in Fig. 2a) to 2004 (green line), with the larger decrease appearing for 1–3 years ice (about 0.45 m) and smaller decline from 4 to 5+ year ice (around 0.2 m). By contrast, a relatively significant sea ice thickness recovery was found in 2005 with smaller thickness increases emerging in younger ice (1–3 years ice, about 0.4 m) and larger increases in older ice (4–5+, approximately 0.7 m). From 2005 till 2008, however, the winter records show a consecutive decrease for the perennial ice age categories (on average 0.80 m), with smaller (roughly 0.5 m) and larger (up to 1.0 m) decline for 2–3 year ice and 4–5+ year ice, respectively. On the other hand, seasonal ice (1-year) shows a small decrease of about 0.3 m. On the whole, the winter record in 2008 presented a much thinner ice for each perennial ice age category compared to those in 2004.

During the ON period, seasonal ice showed a small decline (0.3 m) from about 1.8 m in 2003 to less than 1.5 m for the 2004–2007 record. Then, a slight recovery of roughly 0.2 m was found in 2008. On the contrary, the changes for perennial ice are complex. There was a decrease (0.2 m) through the perennial ice from 2003 to 2004. The decrease was then replenished by an increase from 2005 to 2006 (0.3–0.5 m from 2 through 5+ ice). Afterwards, a moderate thickness decrease appeared across the perennial ice from 2006 until 2008, with declined values amounting to 0.4–0.7 m depending on ice age (on average, 0.6 m).

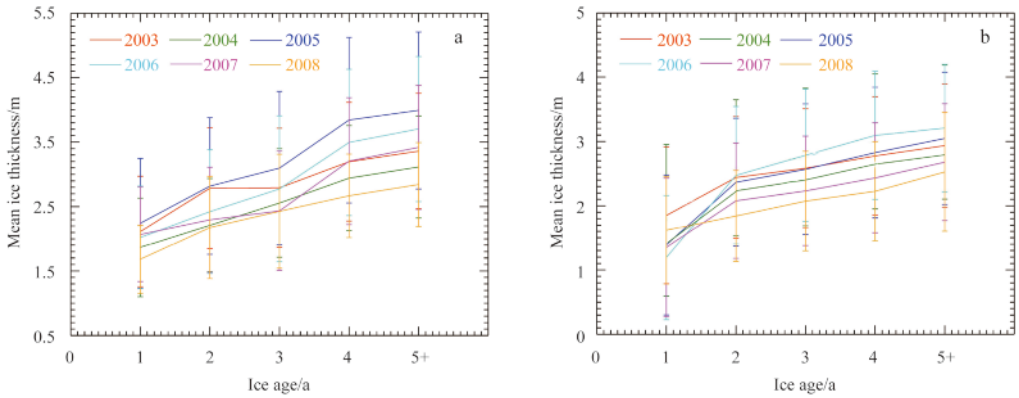

Fig. 6. Mean ICESat-derived thickness of sea ice as a function of sea ice age in the Arctic Ocean during the FMA (a) and ON (b) periods over the 2003–2008 period. Error bars denote standard deviations of sea ice thickness for a given ice age.

4.2 *PIOMAS-based Arctic sea ice thickness changes*

The decadal changes of sea ice thickness as reflected in Fig. 7 were obtained with PIOMAS thickness and ice age data. In total, mean thickness on March of four time periods (1980s (1980–1989), 1990s (1990–1999), 2000s (2000–2009), 2010s (2010–2015)) are presented. Similarly, mean ice thickness of a given ice age was calculated over the Arctic Ocean regime as marked in Fig. 1a.

For the purpose of evaluation, the 5-year mean ICESat sea ice thickness over the 2003–2008 period is added in Fig. 7 (pink line) for comparison. The plot of ICESat thicknesses generally tracks those of PIOMAS in 2000s. Quantitatively, the overall mean difference between ICESat and PIOMAS thickness for all ice age types amounts to (–0.15±0.10) m. The number after "±" denotes standard deviation. To be specific, relatively moderate bias of 0.18 and 0.12 m is found between the ICESat observations and PIOMAS modelled results in two ice age classes, 2-year and 5+ ice, respectively (Fig. 7). Other ice age categories (1, 3, and 4-year), however, reveal smaller differences of no less than 0.1 m, indicating a generally good agreement between the two data fields and lending to a credence of applying PIOMAS thickness for long-term analysis.

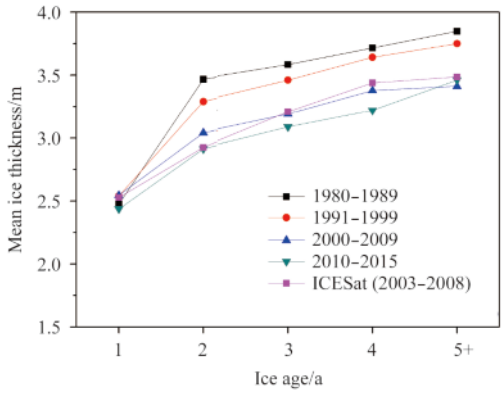

Fig. 7. Variations of PIOMAS-based mean ice thickness on March as a function of ice age.

Overall, Fig. 7 suggests an increasingly decadal decline in mean sea ice thickness regarding perennial ice, of approximately 0.50 m, over the period from 1980s through 2010s. Perennial ice experienced a larger decline of 0.65 m, from 2.75 m (1980s) down to 2.10 m (2010s). By contrast, the thickness of ice older than 5-year (or 5+), has a relatively small drop of roughly by 0.45 m (from 3.0 m to 2.55 m) over the same period. Other ice age categories display a moderate thickness decrease of roughly 0.50 m. Nevertheless, the decadal thickness changes of 1-year ice are negligible.

It is noteworthy that the mean thickness of perennial ice has decreased significantly since the turn of the new century. Based on their magnitude, the thickness fields can be divided into two distinct epoches: the thicker era (1980s and 1990s) and the thin-

ner era (2000s and 2010s). The average changes in sea ice thickness for perennial ice were slight between the two decades of each epoch (around 0.12 m), whereas the changes were significant between the two eras (about 0.55 m). Apart from that, the standard deviation (not shown for clarity) of mean PIOMAS thickness for each ice age category is large and comparable to that of ICESat thickness (Fig. 6), further demonstrating a significant interannual variability of sea ice thickness for various ice age categories.

5 Discussion

5.1 *Short-term variability*

The notable short-term decrease of autumn sea ice thickness for the perennial ice from 2006 to 2008 (Fig. 6) appears mainly to be associated with the extensive Arctic Ocean sea ice loss in summer 2007. The dramatic sea ice retreat during that summer could have preconditioned for a thinner ice cover in autumn due to the effects of albedo-feedback mechanism. Since sea water has a much lower albedo (5%) in comparison with that of sea ice (50%–70%), the decrease of sea ice cover in summer allows more solar radiation to be absorbed. As a result, sea ice bottom-melting process is enhanced. Moreover, superfluous absorbed heat was able to delay the water-freezing procedure in autumn. Both effects are in favor of a thinner sea ice cover in autumn and likely the following winter.

The large standard deviations as indicated by the error bars in Fig. 6 indicate that there is a wide spectrum of sea ice thicknesses corresponding to each ice age category. The exemplary map one for winter 2003 (Fig. 5) provides a clear image of the spatial distribution pattern for Arctic sea ice thickness as well as ice ages. It seems to suggest that, for ice of a given age, when it appears the closer to the northern Greenland and Canadian Archipelago, the thicker it becomes. From the northern Greenland and Canadian Archipelago towards the peripheral seas, such as the Beaufort Sea, Chukchi Sea, East Siberian Sea, and the Laptev Sea, sea ice exhibits a reducing trend in the spatial distribution pattern of ice thickness. Thus, sea ice, even with the same age, may have largely diverse thicknesses depending on areas where it resides.

5.2 *Long-term changes*

5.2.1 *Warming Arctic atmosphere*

What causes the decadal decline in ice thickness? Of course, a warming climate is essential. Serreze et al. (2009) confirmed the emergence of amplified surface atmosphere in Arctic regions during the last decade. NCEP/reanalysis surface air temperature also tells the truth. Compared to 1980s and 1990s, the entire Arctic sea ice regime are becoming warmer for nearly all seasons during the recent two decades (2000s and 2010s) (Fig. 8). In particular, the winter air temperature anomaly (Figs 8c and d) was almost a factor of three in comparison with summer air temperature anomaly (Figs 8a and b) for the two decades of the new century.

Serreze et al. (2009) argued that above-mentioned Arctic amplification in air temperature is largely driven by loss of the sea ice cover, allowing for strong heat transfers from the ocean to the atmosphere. This follows in that while the atmosphere is becoming warmer, it will, in turn, emit strong radiation towards surface. We view these findings as consistent with the emergence

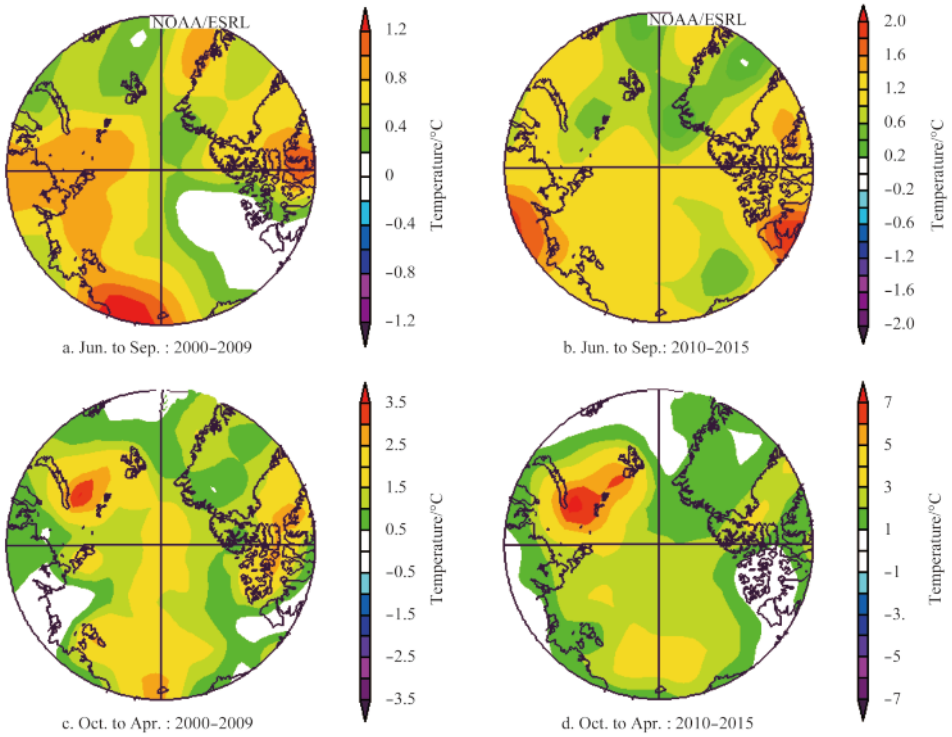

Fig. 8. Mean surface air temperature anomaly (°C), in areas north of 70°N, during summer (June–September, a and b) and winter months (October–April, c and d) over the recent two decades (2000s and 2010s). The mean temperature anomaly for the earlier two decades (1980s and 1990s) is generally negative and not shown. Annual anomaly fields were firstly computed relative to the climatology over the 1980–2010 period. Then, the decadal anomaly (as shown in Figs 8a–d) is estimated by averaging the annual anomaly fields over the corresponding decade.

of delayed freezing and thus thinner sea ice in the Arctic Ocean regions (Stroeve et al., 2014).

Over long-term period, the warmer atmosphere will exert progressive and significant effects on the decline in sea ice thickness but through different ways in different seasons. In winter, warmer atmosphere suppresses the ice growth via slowing the water-frozen process, leaving a thinner-than-normal ice thickness, especially pronounced in regions with seasonal ice in the marginal seas (Laptev Sea, East Siberian Sea, Chukchi Sea, and Beaufort Sea). In summer, warmer atmosphere provides additional heat input into the surface, either assimilated by open water exposed in above marginal seas or melt pond water formed in ice surface. The former heat budget is used to heat the ocean surface in part favorable to bottom melting through heat transportation forced by ocean currents (as analyzed in Section 5.2.2) and/or winds (see Section 5.2.3), whereas the latter budget would cause surface ice melt. Both are conducive to decreases in ice thickness.

5.2.2 *Warming Arctic Ocean*

Previous studies had demonstrated that the effects induced by warming Arctic Ocean on sea ice are more direct. For example, Steele et al.(2010) found summertime sea ice thickness decline due to a warmer Arctic Ocean through absorbing solar radiation induced by albedo-feedback mechanisms. Moreover, hotter Pacific inflows (Woodgate et al., 2010) will also bring extra heat to melting Arctic Ocean sea ice. A model study (Woodgate et al., 2006) argued that ocean current transporting heat penetrates the Bering Strait into the Arctic basin in early springtime would result in a bottom ice melt, leading to a thickness decreases in limited areas of the Chukchi Sea and Beaufort Sea. However, in summer months (June–September) the immediate effectiveness of the heat inject along with Pacific currents in melting sea ice is largely weakened due to the ice-extent retreat to higher north latitudes.

The warm ocean currents effects linked to north Atlantic Water (AW) have far-reached consequences since it took 1.5 years to propagate from the Norwegian Sea to the Fram Strait region, and additional 4.5–5 years to reach the Laptev Sea slope (Polyakov et al., 2005). Warm AW (Steele et al., 2008) entering into the Arctic Ocean release additional energy, which is partly used to melt sea ice. Analysis of modern and historical observations (Polyakov et al., 2010) demonstrated that the temperature of the intermediate-depth (150–900 m) AW of the Arctic Ocean had increased in recent decades. The warming is associated with a substantial (up to 75–90 m) shoaling of the upper AW boundary in the central Arctic Ocean and weakening of the Eurasian Basin upper-ocean stratification. Moreover, modelled results (Polyakov et al., 2010) suggest that the warming AW during the last 50 years, that caused a heat flux increase of 0.5 W/m^2, contributed to a thickness loss of 28–35 cm comparable to estimates based on fast ice observations of 29 cm.

5.2.3 *Role of summer winds*

There were studies that have investigated the role of summer and winter winds in the rapid decrease of summer sea ice extent. They found the effect of summer winds in pushing sea ice edge from coastal slope across the North Pole towards the Fram Strait region. While in this study we show the role of summer winds in transporting warmer Arctic Ocean surface water into deep ocean, facilitating bottom melting and thus thinner ice cover and/or decreased ice concentration.

Many studies related the albedo-feedback mechanism to the recently observed frequent dramatic retreat in Arctic Ocean sea ice cover during summer (Perovich et al., 2007, 2008; Zhang et al., 2008). In particular, Perovich et al. (2008) presented observational evidence of a distinct bottom melt up to 2 m around the Beaufort Sea just following the 2007 dramatic summer ice loss in the Arctic Ocean. But a puzzle remains: what is the primary driver of transporting such warmer surface water in marginal seas into deep Arctic Ocean capped by sea ice. If warm surface water is effectively transport into deep ocean, the bottom melt of sea ice will be strengthened.

In this study, we attempted to examine the role of summer winds in transporting warm surface water in marginal seas into deep ocean. The summer winds anomaly during the ICESat period (2003–2008) were screened and a characteristic map is shown in Fig. 9. Strong southerly wind anomalies (>3.5 m/s) over East Siberian Sea, Chukchi Sea, and Beaufort Sea (hereafter referred to as the ES-CS-BS seas) is evident in summer 2007. With this kind of anomalous winds, two aspects of effects on sea ice are expected. On one hand, it pushes the sea ice towards north of Canadian Archipelago and towards the Fram Strait where ice flows out of the Arctic Ocean. The results of this circulation pattern are the decrease of sea ice extent (Ogi et al., 2010), which allows more solar radiation to be absorbed and, in turn, helps to melting sea ice in limited regions adjacent to sea ice edge. On the other hand, the anomalous southerly winds favor the transport of the warm ocean surface water of the peripheral seas into deep Arctic Ocean regions, facilitating bottom-melting of sea ice there. The observed distinguished thinner ice in autumn/winter period of 2007/08 following the summer 2007 (as shown in Fig. 6) seems to support the idea that southerly summer winds in ES-CS-BS seas, to a certain degree, contribute to the thickness decline of the Arctic Ocean sea ice.

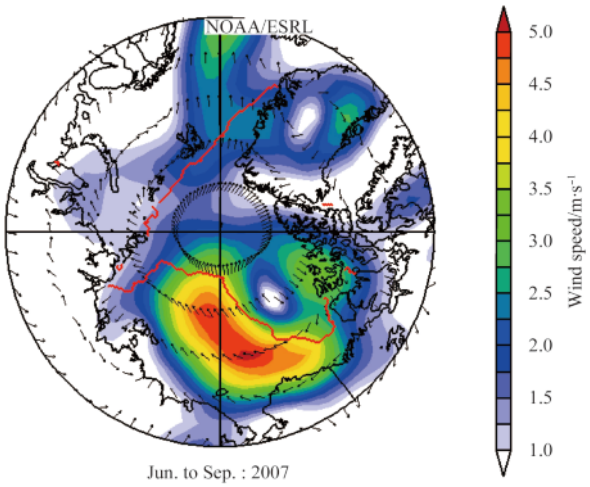

Fig. 9. Mean summer (June–September) winds anomaly in 2007 with September ice extent overlaid. Arrows refer to the direction of wind anomaly vectors and background color indicates the magnitude of wind speed anomaly. A distinct wind anomaly towards north latitudes is found in Pacific sector (the zone occupied by yellow-to-red color) where sea ice loss is pronounced in this summer.

Over the decadal timescale we also found a similar function of summer winds in prompting broad ice thickness decline through northerly pushing warm water into deep basin. During

summer of 1980s and 1990s sea ice occupied the most part of the Arctic Ocean with open water appearing only in a long and narrow belt embracing the bulk of the sea ice (as shown in Fig. 10a, the open water regions between coast and the median ice extent (red line) is very limited). Northerly or northeasterly winds anomaly were popular in the 1980s and 1990s which favors the outspread of summer ice toward neighboring ES-CS-BS seas and also restricts the surface water that warmed by solar radiation to be transported to the northern sea ice region. By contrast, the wind anomaly was significantly reversed in 2000s and heat stored in surface water of ES-CS-BS seas can be effectively carried into the north latitudes where sea ice cover prevails. The southerly winds are responsible for northwardly spreading the substantial heat input in ES-CS-BS seas into the broad and deep Arctic Ocean. Therefore, in addition to the influences of a warmer atmosphere, summer winds also played an important role in bringing about a thinner ice over all ice age categories. In 2010s, the summer winds anomaly was nearly close to the climatology and may contribute less to a thinner ice. Compared to 2000s, however, sea ice thickness for perennial ice did not recover in 2010s with further decreases being found (Fig. 7). This continued downward trend in thickness is likely maintained by an even warmer Arctic climate (Fig. 8). To be noteworthy, the summer ice extent in 2010s reduced even more (Fig. 10d) compared to that in 2000s (Fig. 10c), thereby if the winds anomaly like the 2000s reappear another catastrophic ice extent loss in summer and dramatic ice thickness decline will be on the stage again.

As the Arctic sea ice become increasing thinner, it may have

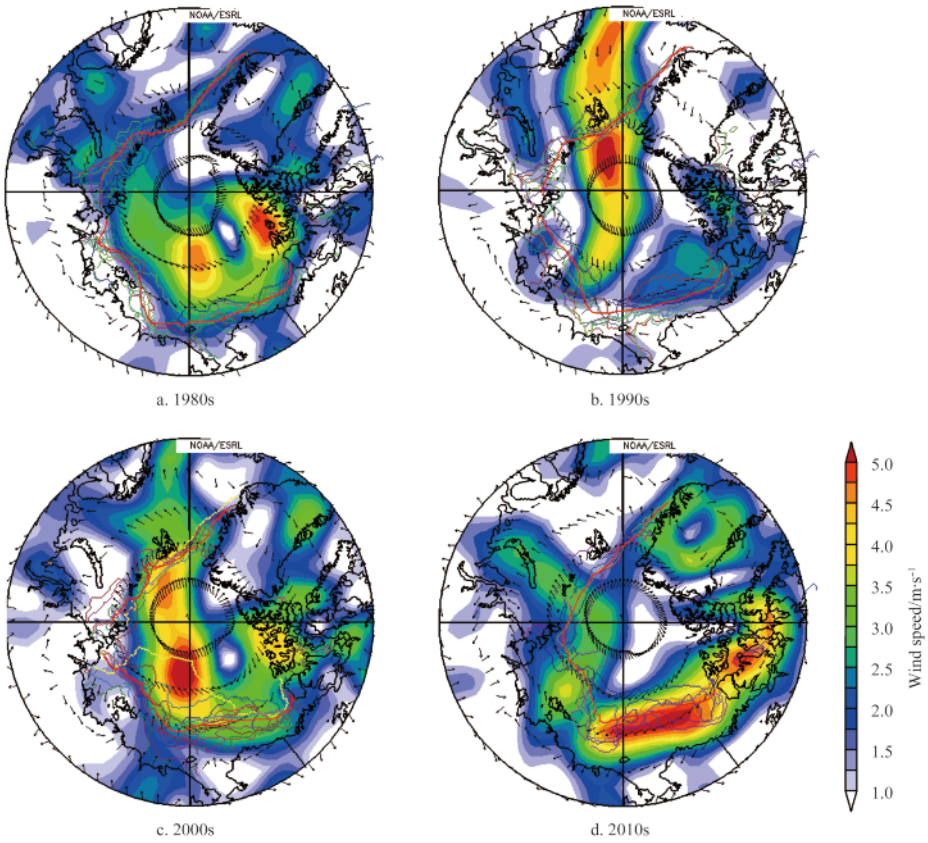

Fig. 10. As in Fig. 9 but for the averaged summer wind anomaly over past four decades, including 1980s (a), 1990s (b), 2000s (c), and 2010s (d). The overlaid red bold line represents the median ice extent over the corresponding decade. The continued retreat of the sea ice extent towards higher north latitudes is obvious from 1980s through 2010s.

entered into a state of particularly vulnerable to anomalous oceanic and atmospheric forcing. Since there is no sign that there will be a sharp reversal to the pre-1980s climate status, a thinner Arctic Ocean sea ice cover is expected in near future. Yang et al.(2014) presented a better way to assimilate NSIDC SSM/I ice concentration and SMOS sea ice thickness in order to improve the quality of modelled results of a coupled sea ice-ocean model. This is an intriguing experiment and their results may be useful in our future study based on more accurate modelled ice thickness.

6 Conclusions

The overall thinning trend in the Arctic Ocean sea ice has been well documented in previous studies (Maslanik et al., 2007; Giles et al., 2008; Haas et al., 2008; Rothrock et al., 2008; Kwok et al., 2009; Kwok and Rothrock, 2009). The extensive loss of multiyear ice especially the older/thicker component is considered as one of the most important aspect of the decreases in sea ice thickness (Maslanik et al., 2007). Besides, in this study we found a thinning for each ice category not only evidenced by short term satellite data but also by long term model results. This change is vital, in conjunction with retreat in multiyear ice coverage, contributing to a significant sea ice volume and mass loss in the Arctic Ocean.

In this study, the ICESat-derived sea ice thicknesses were used to examine the high interannual variability of the sea ice thickness for each ice age category, while PIOMAS model data were explored to investigate the decadal changes. The ICESat-

based results reflect a clear thickness decline of 0.5–1.0 m (with older ice reducing more) in winter (FMA) period in 2008, compared to a local maximum thickness in winter 2005. The thickness decline in perennial ice of 0.6–0.8 m depending ice age during autumn (ON) period is also significant compared to that of 2006. The 1-year ice did not show significant variability during the ICESat period. On the other hand, PIOMAS ice thickness, which on average agrees well with in-phase ICESat results, shows a continued decline in thickness of about 0.5 m for all perennial ice categories over the past four decades since 1980s. Also, PIOMAS-based sea ice thickness changes of 1-year ice are not obvious.

The long term thinning trend from 1980s through 2010s for all perennial ice types as reflected in our PIOMAS-based results can be predominantly attributable to the amplified warming circumstance (atmosphere and ocean) both in winter and summer seasons in the northern hemisphere. In addition, we inspected the role of summer winds which could transport warm water (heat input absorbed from solar radiation and/or atmosphere and stored in upper surface water) deep into the Arctic Ocean where ice caps the surface. It is suggested that under the situations of strong anomalous southerly winds, heat deposited in the open water in Pacific sector may be conveyed into a broader Central Arctic Ocean and partly used in ice bottom melting. As a result, ice thickness for perennial ice may be reduced significantly.

References

Alexeev V A, Ivanov V V, Kwok R, et al. 2013. North Atlantic warming and declining volume of arctic sea ice. The Cryosphere Discussions, 7(1): 245–265

Comiso J C, Parkinson C L, Gersten R, et al. 2008. Accelerated decline in the Arctic sea ice cover. Geophysical Research Letters, 35(1): doi: 10.1029/2007GL031972

Deser C, Teng Haiyan. 2008. Evolution of Arctic sea ice concentration trends and the role of atmospheric circulation forcing, 1979–2007. Geophysical Research Letters, 35(2): doi: 10.1029/2007GL032023

Fetterer F, Knowles K, Meier W, et al. 2002. Sea Ice Index. Boulder, Colorado USA: National Snow and Ice Data Center, doi: 10.7265/N5QJ7F7W

Giles K A, Laxon S W, Ridout A L. 2008. Circumpolar thinning of Arctic sea ice following the 2007 record ice extent minimum. Geophysical Research Letters, 35(22): doi: 10.1029/2008GL035710

Haas C, Pfaffling A, Hendricks S, et al. 2008. Reduced ice thickness in Arctic Transpolar Drift favors rapid ice retreat. Geophysical Research Letters, 35(17): doi: 10.1029/2008GL034457

Johannessen O M, Bengtsson L, Miles M W, et al. 2004. Arctic climate change: observed and modelled temperature and sea-ice variability. Tellus A, 56(4): 328–341

Kalnay E, Kanamitsu M, Kistler R, et al. 1996. The NCEP/NCAR 40-year reanalysis project. Bulletin of the American Meteorological Society, 77(3): 437–471

Kwok R, Cunningham G F. 2008. ICESat over Arctic sea ice: Estimation of snow depth and ice thickness. Journal of Geophysical Research: Oceans (1978-2012), 113(C8): doi: 10.1029/2008JC004753

Kwok R, Cunningham G F, Wensnahan M, et al. 2009. Thinning and volume loss of the Arctic Ocean sea ice cover: 2003–2008. Journal of Geophysical Research: Oceans (1978–2012), 114(C7): doi: 10.1029/2009JC005312

Kwok R, Rothrock D A. 2009. Decline in Arctic sea ice thickness from submarine and ICESat records: 1958–2008. Geophysical Research Letters, 36(15): doi: 10.1029/2009GL039035

Laxon S, Peacock N, Smith D. 2003. High interannual variability of sea ice thickness in the Arctic region. Nature, 425(6961): 947–950

Markus T, Stroeve J C, Miller J. 2009. Recent changes in Arctic sea ice melt onset, freezeup, and melt season length. Journal of Geophysical Research: Oceans (1978–2012), 114(C12): doi: 10.1029/2009JC005436

Maslanik J A, Fowler C, Stroeve J, et al. 2007. A younger, thinner Arctic ice cover: Increased potential for rapid, extensive sea-ice loss. Geophysical Research Letters, 34(24): doi: 10.1029/2007GL032043

Maslanik J, Stroeve J, Fowler C, et al. 2011. Distribution and trends in Arctic sea ice age through spring 2011. Geophysical Research Letters, 38(13): doi: 10.1029/2011GL047735

Ogi M, Yamazaki K, Wallace J M. 2010. Influence of winter and summer surface wind anomalies on Summer Arctic sea ice extent. Geophysical Research Letters, 37(7): doi: 10.1029/2009GL042356

Perovich D K, Light B, Eicken H, et al. 2007. Increasing solar heating of the Arctic Ocean and adjacent seas, 1979–2005: Attribution and role in the ice-albedo feedback. Geophysical Research Letters, 34(19): doi: 10.1029/2007GL031480

Perovich D K, Richter-Menge J A, Jones K F, et al. 2008. Sunlight, water, and ice: Extreme Arctic sea ice melt during the summer of 2007. Geophysical Research Letters, 35(11): doi: 10.1029/2008GL034007

Polyakov I V, Beszczynska A, Carmack E C, et al. 2005. One more step toward a warmer Arctic. Geophysical Research Letters, 32(17): doi: 10.1029/2005GL023740

Polyakov I V, Timokhov L A, Alexeev V A, et al. 2010. Arctic Ocean warming contributes to reduced polar ice cap. Journal of Physical Oceanography, 40(12): 2743–2756

Rigor I G, Wallace J M. 2004. Variations in the age of Arctic sea-ice and summer sea-ice extent. Geophysical Research Letters, 31(9): doi: 10.1029/2004GL019492

Rothrock D A, Percival D B, Wensnahan M. 2008. The decline in arctic sea-ice thickness: Separating the spatial, annual, and interannual variability in a quarter century of submarine data. Journal of Geophysical Research: Oceans (1978–2012), 113(C5): doi: 10.1029/2007JC004252

Schröder D, Feltham D L, Flocco D, et al. 2014. September Arctic sea-ice minimum predicted by spring melt-pond fraction. Nature Climate Change, 4(5): 353–357

Schweiger A, Lindsay R, Zhang Jinlun, et al. 2011. Uncertainty in modeled Arctic sea ice volume. Journal of Geophysical Research: Oceans (1978–2012), 116(C8): doi: 10.1029/2011JC007084

Serreze M C, Barrett A P, Stroeve J C, et al. 2009. The emergence of surface-based Arctic amplification. The Cryosphere, 3(1): 11–19

Shimada K, Kamoshida T, Itoh M, et al. 2006. Pacific Ocean inflow: Influence on catastrophic reduction of sea ice cover in the Arctic Ocean. Geophysical Research Letters, 33(8): doi: 10.1029/2005GL025624

Spreen G. 2008. Satellite-based estimates of Sea ice volume flux: applications to the fram Strait Region [dissertation]. Hamburg: Universität Hamburg

Steele M, Ermold W, Zhang Jinlun. 2008. Arctic Ocean surface warming trends over the past 100 years. Geophysical Research Letters, 35(2): doi: 10.1029/2007GL031651

Steele M, Zhang Jinlun, Ermold W. 2010. Mechanisms of summertime upper Arctic Ocean warming and the effect on sea ice melt. Journal of Geophysical Research: Oceans (1978–2012), 115(C11): doi: 10.1029/2009JC005849

Stroeve J C, Markus T, Boisvert L, et al. 2014. Changes in Arctic melt season and implications for sea ice loss. Geophysical Research Letters, 41(4): 1216–1225

Tschudi M, Fowler C, Maslanik J. 2014. EASE-grid Sea Ice age. Version 2. [indicate subset used]. Boulder, Colorado USA: NASA National Snow and Ice Data Center Distributed Active Archive Center, doi: 10.5067/1UQJWCYPVX61

Vinnikov K Y, Robock A, Stouffer R J, et al. 1999. Global warming and Northern Hemisphere sea ice extent. Science, 286(5446): 1934–1937

Warren S G, Rigor I G, Untersteiner N, et al. 1999. Snow depth on Arctic sea ice. Journal of Climate, 12(6): 1814–1829

Woodgate R A, Aagaard K, Weingartner T J. 2006. Interannual changes in the Bering Strait fluxes of volume, heat and freshwater between 1991 and 2004. Geophysical Research Letters, 33(15): doi: 10.1029/2006GL026931

Woodgate R A, Weingartner T, Lindsay R. 2010. The 2007 Bering Strait oceanic heat flux and anomalous Arctic sea-ice retreat. Geophysical Research Letters, 37(1): doi: 10.1029/2009GL041621

Yang Qinghua, Losa S N, Losch M, et al. 2014. Assimilating SMOS sea ice thickness into a coupled ice-ocean model using a local SEIK filter. Journal of Geophysical Research: Oceans, 119(10): 6680–6692

Yi Donghui, Zwally J. 2014. Arctic Sea Ice freeboard and thickness [indicate subset used]. Boulder, Colorado USA: NASA DAAC at the National Snow and Ice Data Center

Zhang Junlun, Lindsay R, Steele M, et al. 2008. What drove the dramatic retreat of arctic sea ice during summer 2007?. Geophysical Research Letters, 35(11): doi: 10.1029/2008GL034005

Zhang Jinjun, Rothrock D A. 2003. Modeling global sea ice with a thickness and enthalpy distribution model in generalized curvilinear coordinates. Monthly Weather Review, 131(5): 845–861

Zwally H J, Schutz B, Abdalati W, et al. 2002. ICESat's laser measurements of polar ice, atmosphere, ocean, and land. Journal of Geodynamics, 34(3-4): 405–445

Zwally H J, Yi Donghui, Kwok R, et al. 2008. ICESat measurements of sea ice freeboard and estimates of sea ice thickness in the Weddell Sea. Journal of Geophysical Research: Oceans (1978–2012), 113(C2): doi: 10.1029/2007JC004284